Effect of gradient production on scalar fluctuations in decaying grid turbulence

L. Danaila,[1] and L. Mydlarski[2]
[1]*IRPHE, 49 Rue F. Joliot-Curie, Boîte Postale 146, 13384 Marseille Cedex 13, France; and LET, University of Poitiers, 40 Avenue du Recteur Pineau, 86022, Poitiers, France*
[2]*Department of Mechanical Engineering, McGill University, 817 Sherbrooke Street West, Montréal, Québec, Canada H3A-2K6*
(Received 19 February 2001; published 27 June 2001)

A generalized form of Yaglom's equation, in which the effect of turbulent production of temperature fluctuations is taken into account, is derived. The modified Yaglom equation (which extends the work of Danaila *et al.* [J. Fluid Mech. **391**, 359 (1999)] to incorporate the effects of decay *and* production) is compared with experimental data. The flow under consideration is decaying grid turbulence with an imposed mean temperature gradient (Mydlarski and Warhaft [J. Fluid Mech. **358**, 135 (1998)]). The agreement between theory and experiment is good and the effects of nonhomogeneities in the flow are small.

DOI: 10.1103/PhysRevE.64.016316 PACS number(s): 47.27.Ak, 47.27.Jv, 47.27.Te

I. INTRODUCTION

The properties of a turbulent field θ can be studied by considering the nth-order moments of its increments over a separation $\vec{r}$. These moments are more commonly called structure functions and are defined by $S_n=\langle(\Delta\theta)^n\rangle\equiv\langle(\theta(\vec{x}+\vec{r})-\theta(\vec{x}))^n\rangle$. In 1949, Yaglom [1], following the notions of Kolmogorov [2,3], developed a relationship between the second-order moments of the scalar increment over an interval r in the longitudinal (x_1) direction, $\langle(\Delta\theta(r))^2\rangle$, and the third-order mixed moments, $\langle\Delta u_1(r)(\Delta\theta(r))^2\rangle$, also in the longitudinal direction. Here u_1 is the component of the velocity fluctuation in the streamwise (i.e., longitudinal) direction, θ is the scalar fluctuation and $\Delta\theta(r)\equiv\theta(x_1+r)-\theta(x_1)$. This relation, called Yaglom's equation, is given by

$$-\langle\Delta u_1(\Delta\theta)^2\rangle+2\kappa\frac{d}{dr}\langle(\Delta\theta)^2\rangle=\frac{4}{3}\langle\epsilon_\theta\rangle r. \tag{1}$$

The rate of destruction of the scalar variance, $\langle\epsilon_\theta\rangle$, is defined as

$$\langle\epsilon_\theta\rangle\equiv\kappa\left\langle\frac{\partial\theta}{\partial x_i}\frac{\partial\theta}{\partial x_i}\right\rangle, \tag{2}$$

where κ is the scalar molecular diffusivity, and angular brackets denote an average in time. Equation (1) is derived within the framework of Kolmogorov [2,3], that is to say, assuming a cascade which is universal and locally isotropic for small enough scales and large enough Reynolds numbers.[1]

Writing Eq. (1) as $A+B=C$, term C (directly proportional to $\langle\epsilon_\theta\rangle$), is associated with the transfer of scalar variance at a scale r. Equation (1) indicates that the mean scalar variance transferred at a scale r is transferred by both turbulent advection (term A) and molecular diffusion (term B). Equation (1) could also be used as an alternate means of (experimentally) determining $\langle\epsilon_\theta\rangle$, since the second- and third-order moments could be inferred from hot- and cold-wire measurements, via Taylor's hypothesis (given a locally isotropic and homogeneous flow).

At small Reynolds numbers, the sum $A+B$ never balances C, except for the smallest scales (e.g., $A+B=C$ for $r/\eta\lesssim 5$ at $R_\lambda=66$ [4][2]). (In the limit of small separations, A tends to 0 and $B=C$, as will be discussed shortly.)

For intermediate Reynolds numbers ($100<R_\lambda<500$), Kolmogorov's equation and Yaglom's equation are not satisfied for moderate to large scales (e.g., Refs. [5–7]). Equation (1) is only found to be satisfied up to a maximum scale which depends on the Reynolds number. It is never verified at the largest scales.

This discrepancy is the subject of this work. Though derived from a relation which is satisfied (the advection-diffusion equation), Yaglom's equation is not satisfied. This can only occur if the derivation does not take into account the phenomena present in nonisotropic flows, such as the one under consideration. In this work, the phenomena are the decay of the turbulence and the production of scalar fluctuations by a mean scalar gradient.

In order to account for the role of the large scales, Frisch [8] derived a version of Kolmogorov's equation which included a random forcing term (acting only at large scales). A detailed study of Kolmogorov's equation was presented by Hill [9], where the nonstationarity of decaying flows was taken analytically into account, but no quantitative verification was given. The influence of large scales on the statistical properties of the cascade has also been addressed by Lindborg [10] and Moisy *et al.* [11].

[1]Equation (1) is the scalar field analog of Kolmogorov's equation: $[-\langle(\Delta u_1)^3\rangle+6\nu(d/dr)\langle(\Delta u_1)^2\rangle=\frac{4}{5}\langle\epsilon\rangle r]$, which applies to the velocity field. Both Kolmogorov's and Yaglom's equations are particularly relevant to the study of turbulence since they are the only known relations derivable from conservation of momentum and energy, respectively.

[2]$R_\lambda\equiv(u_{rms}\lambda/\nu)$, where u_{rms} is the root-mean-square value of the longitudinal velocity fluctuation, ν is the kinematic viscosity, and λ is the Taylor microscale, defined as $\lambda\equiv[\langle u_1^2\rangle/\langle(\partial u_1/\partial x_1)^2\rangle]^{1/2}$.

Recently, it was shown [4] that, in grid turbulence, the nonstationarity plays a capital role in the correct balance of Eq. (1) and Kolmogorov's equation. This was demonstrated by an analysis of the transfer of the scalar moments that retained the large-scale influence while simultaneously applying the concepts of local homogeneity and isotropy to scales much smaller than those at which the scalar is injected. Thus an accurate quantitative study of the transfer of the moments through the scales has to properly consider the large scale influence. In particular, Danaila *et al.* [4] showed that violations of Kolmogorov's and Yaglom's equations imply a correlation between the large-scales of a turbulent flow (where the fluctuations are generated) and the small scales (where they are destroyed). To further elucidate these correlations, Danaila *et al.* developed generalizations of Kolmogorov's equation and Yaglom's equation that accounted for the effects of nonstationarity[3] of the second-order moments. They are

$$-\langle(\Delta u_1)^3\rangle+6\nu\frac{d}{dr}\langle(\Delta u_1)^2\rangle-3\frac{U_1}{r^4}\int_0^r y^4\frac{\partial}{\partial x_1}\langle(\Delta u_1)^2\rangle dy = \frac{4}{5}\langle\epsilon\rangle r, \tag{3}$$

and

$$-\langle\Delta u_1(\Delta\theta)^2\rangle+2\kappa\frac{d}{dr}\langle(\Delta\theta)^2\rangle-\frac{U_1}{r^2}\int_0^r y^2\frac{\partial}{\partial x_1}\langle(\Delta\theta)^2\rangle dy = \frac{4}{3}\langle\epsilon_\theta\rangle r, \tag{4}$$

respectively. In Eq. (3), $\langle\epsilon\rangle$ is the mean dissipation rate of the turbulent kinetic energy, and y is a dummy variable.

These predictions were found to agree well with experimental data of homogeneous, isotropic, decaying, grid-generated turbulence. (Isotropic scalar fluctuations were generated by means of a ''mandoline'' [12] placed downstream of the grid.) The deviation of the left-hand side of Eq. (1) from $\frac{4}{3}\langle\epsilon_\theta\rangle r$ was found to be dictated by the effect of the non-stationarity of the second-order moments. The deviation was equal to $(U_1/r^2)\int_0^r y^2(\partial/\partial x_1)\langle(\Delta\theta)^2\rangle dy$—the third term from the left in their modified Yaglom's equation [Eq. (4)].

Given the success of the method proposed by Danaila *et al.*, it is reasonable to extend it to more complex flows. The objective of this paper is to apply this method to flows with mean scalar gradients (in addition to nonstationarities). Specifically, the method will be applied to decaying grid-generated turbulence with an imposed mean temperature gradient. We take into account the role of the large scales (by accounting for the mean scalar gradient $\vec{G}$), and we assume that the terms appearing at relatively small scales, such as terms A and B, are isotropic. [We call this range of scales the restricted scaling range (RSR) and define it to be the range of scales from the Kolmogorov microscale $(\eta\equiv(\nu^3/\langle\epsilon\rangle)^{1/4})$ to the largest scale where $\langle\Delta u_1(\Delta\theta)^2\rangle$ remains proportional to r. In the RSR, the constant of proportionality is not necessarily equal to $-\frac{4}{3}\langle\epsilon_\theta\rangle$ because of the other effects we consider in this paper.] The obtained results will be compared with the experimental data of Mydlarski and Warhaft [7].

Before proceeding, we point out one aspect of flows with mean scalar gradients. Assuming isotropy, the scalar ''dissipation'' rate $\langle\epsilon_\theta\rangle$ can be estimated as

$$\langle\epsilon_\theta\rangle_{iso}\equiv 3\kappa\langle(\partial_{x_1}\theta)^2\rangle. \tag{5}$$

Equation (5) is often used in experiments involving passive scalars since the right hand side is readily measured. If the assumption of isotropy is indeed valid, then $\langle\epsilon_\theta\rangle$ and $\langle\epsilon_\theta\rangle_{iso}$ are equal. Hereafter, we will clearly differentiate between $\langle\epsilon_\theta\rangle$ and its isotropic form, $\langle\epsilon_\theta\rangle_{iso}$, given by Eq. (5).

Given that

$$\lim_{r\to 0}2\kappa\frac{d}{dr}\langle(\Delta\theta)^2\rangle=\lim_{r\to 0}2\kappa\frac{d}{dr}\left\langle\frac{(\Delta\theta)^2}{r^2}r^2\right\rangle = 2\kappa\langle(\partial_{x_1}\theta)^2\rangle\frac{d}{dr}(r^2)=\frac{4}{3}\langle\epsilon_\theta\rangle_{iso}r, \tag{6}$$

we see that Eq. (1) reduces to $B=C$ in the limit $r\to 0$. In this limit, term A is two orders of magnitude smaller and therefore negligible. Consequently, at the smallest scales, Eq. (1) is consistent with the isotropic definition of the dissipation rate, $\langle\epsilon_\theta\rangle_{iso}$. This result is to be expected since Yaglom's equation was derived assuming isotropy. Alternatively, Yaglom's equation will be verified for very small scales if and only if $\langle\epsilon_\theta\rangle=\langle\epsilon_\theta\rangle_{iso}$.

Experimental and numerical studies have shown [7,13–16] that, in any turbulent flow with an imposed mean scalar gradient $(\vec{G})$, the turbulent scalar field is anisotropic, even for the smallest scales and large Reynolds numbers. A relevant example of this anisotropy is that the temperature derivative variance in the direction parallel to $\vec{G}$ is different than it is in the other directions [7,14,15]. In particular, if one defines the x_3 direction as parallel to $\vec{G}$, it was shown that the variance of the scalar derivative along the x_3 direction is larger than the variance of the derivative along a perpendicular direction (i.e., x_1 or x_2). For example,

$$R_{x_3x_1}=\langle(\partial_{x_3}\theta)^2\rangle/\langle(\partial_{x_1}\theta)^2\rangle\approx 1.2-1.4. \tag{7}$$

[3]In decaying grid-generated turbulence, this effect can be interpreted as a nonstationarity in a coordinate system that moves with the mean velocity of the flow. In a fixed coordinate system, it can be interpreted as a large-scale nonhomogeneity. This is, in fact, how this effect is presented in the equations that follow.

In the flow under consideration, $R_{x_3x_1}=1.4$. Therefore, in this work we use $\langle \epsilon_\theta \rangle \equiv 3.4\kappa\langle(\partial_{x_1}\theta)^2\rangle$.[4]

The implication is that the mean scalar gradient affects the mixing down to the smallest scales, thus violating the concept of local isotropy. Therefore, in flows with mean scalar gradients, Yaglom's equation will not be verified at *any* scale due to the scalar anisotropy present in such flows.

II. APPARATUS

The present results consist of a series of experiments performed under conditions similar to those of Mydlarski and Warhaft [7]. The discussion of the apparatus and the flow characteristics will therefore only summarize what is given in the aforementioned paper.

The experiments were conducted in a $0.91\times0.91\times9.1$ m^3 low-speed, low-background-turbulence wind tunnel in the Department of Mechanical and Aerospace Engineering at Cornell University. This tunnel was described by detail by Yoon and Warhaft [17]. The standard biplanar grids used to generate the turbulence in Yoon and Warhaft were replaced by an active grid which followed the design of Makita [18].

The use of an active grid permits the achievement of much higher turbulent Reynolds numbers than by means of standard ''passive'' grids. Active grids were used to achieve high-Reynolds-number, homogeneous, quasi-isotropic, decaying turbulence in average size wind tunnels [6,7,18] and, in particular, they were used to study the effects of variations in Reynolds number on the turbulent velocity field [6] and variations in Péclet number on the turbulent scalar field [7]. The active grid is composed of round grid bars to which triangular agitator wings are attached. The grid bars are rotated by means of stepper motors located on the outside of the grid. The active grid, tuned and operated in a manner to achieve good homogeneity of the flow, was described in detail in the papers of Mydlarski and Warhaft [6,7].

The mean temperature gradient was produced by means of a *toaster*, first introduced by Sirivat and Warhaft [19]. It consists of a set of parallel, differentially heated ribbons located at the entrance to the wind tunnel plenum chamber, (see Sirivat and Warhaft [19] or Yoon and Warhaft [17], for a schematic). The air entering the plenum chamber is heated as it passes over the ribbons. As it continues though the honeycombs, screens, etc. in the plenum, the (momentum and thermal) wakes of the heater ribbons are smoothed out. The result is a mean temperature gradient in the quasilaminar flow upstream of the grid. The electric current passing through each heater element is iteratively adjusted so that a linear temperature gradient results in the wind tunnel test section (downstream of the grid). The resulting mean temperature gradient is in the x_3 direction. (The mean flow is in the x_1 direction.) The velocity fluctuations (generated by the grid) act against the mean temperature gradient to produce thermal fluctuations. In this work, the ratio of production of turbulent velocity fluctuations by the mean scalar gradient to the dissipation of turbulent kinetic energy was -3.44% (at $x/M=62$—the point the furthest downstream at which measurements were made. This is also the point where the dissipation was minimum, and thus the point where the effects of the stratification will be most significant. M is the mesh length of the grid.) Thus the temperature fluctuations can be considered to be passive.

We additionally point out that in homogeneous, isotropic, decaying wind-tunnel turbulence, an imposed linear mean temperature gradient will not decay [20]. This is an idealization, which is closely achieved in reality [19] if the tunnel width is much larger than the integral scale of the turbulence. Assuming that the mechanical to thermal time scale is unity, it can be shown [17] that, in such a flow, the scalar variance should be proportional to x_1^{2-n}, where n is the decay exponent of the turbulence [i.e., $\langle u_1^2\rangle/U_1^2 \propto (x_1/M)^n$]. In grid turbulence, $n\approx1.2-1.3$ and passive scalar fluctuations should grow as $(x_1/M)^{0.7-0.8}$. As described by Mydlarski and Warhaft [7], an artifact of the active grid is a large integral scale and therefore a slight decay of the scalar gradient in the streamwise direction $[(\partial T/\partial x_1)/(\partial T/\partial x_3)<0.1]$. Since the mean scalar gradient decays, so does the production of scalar fluctuations. As a result, the variance does not grow with a power law dependence on x_1/M. In fact, it reaches a maximum at $x_1/M=37$. However, when appropriately nondimensionalized by the local mean temperature gradient and a length scale [i.e., $\langle\theta(x_1)^2\rangle/(\beta(x_1)M)^2$], the scalar variance increases as $(x_1/M)^{0.7}$ (not shown), as it should for passive scalar fluctuations generated by a linear mean temperature gradient.

The velocity fluctuations were measured using a TSI 1241 X-wire probe. 3.05-μm-diameter tungsten wires with a length to diameter ratio of approximately 200 were used. They were operated with an overheat ratio of 1.8 using Dantec 55M01 constant-temperature hot-wire anemometers. The X wires were calibrated following the method of Browne, Antonia, and Chua [21], which used an effective angle between the wire and the streamwise direction. Following the method of Lienhard [22], compensation of the velocity measurements for temperature fluctuations was made by means of a modified King's law with temperature-dependent coefficients. The two wires comprising the X wire were separated by 0.5 mm. The cold wire (to measure the temperature fluctuations) was placed 0.5 mm away from the X wire.

The temperature fluctuations were measured using a TSI 1210 single wire probe. Platinum cold-wires of 0.63-μm diameter were used. The ratio of the etched length of the wire to its diameter was approximately 550, and the spacing between the prongs was at least three times the etched length. The probe current in the fast-response dc temperature bridges (based on the design of Haughdal and Lienhard [23]) was approximately 250 μA.

A thorough discussion of the frequency response of the probes and the cold-wire thermometers was given by Mydlarski and Warhaft [7]. Also addressed was the optimal choice of cold wire length given the competing effects of spatial resolution and conduction between the cold-wire and its prongs. The discussion (not repeated here) showed that

[4] $\langle \epsilon_\theta \rangle \equiv (1+R_{x_2x_1}+R_{x_3x_1})\kappa\langle(\partial_{x_1}\theta)^2\rangle$, and due to the nature of the flow, $R_{x_2x_1}=1$ (see Mydlarski and Warhaft [7]).

TABLE I. Flow parameters. M represents the mesh length of the active grid, 0.114 m (=4.5 in.). g represents the acceleration due to gravity, 9.81 m/s^2.

Mean speed (m/s)	5.43
x_1/M	62
T_o (°C)	28.7
β (°C/m)	15.6
ν (m^2/s)	16×10^{-6}
κ (m^2/s)	22.5×10^{-6}
u_{rms} (m/s)	0.348
$\langle\epsilon\rangle$ $[=15\nu\langle(\partial u_1/\partial x_1)^2\rangle]$ (m^2/s^3)	0.278
l $(=0.9u_{rms}^3/\langle\epsilon\rangle)$ (m)	0.136
R_λ $\{=\langle u^2\rangle[15/(\nu\langle\epsilon\rangle)]^{1/2}\}$	222
R_l $(=u_{rms}l/\nu)$	2960
η $[=(\nu^3/\langle\epsilon\rangle)^{1/4}]$ (mm)	0.348
l/η	391
θ_{rms} (°C)	1.91
$\langle\epsilon_\theta\rangle$ $[=3.4\kappa\langle(\partial\theta/\partial x_1)^2\rangle]$ (°C^2/s)	4.23
l_θ $(=\theta_{rms}/\beta)$ (m)	0.122
$\langle u_3\theta\rangle$ (°C m/s)	-0.295
$g\langle u_3\theta\rangle/(T_o\langle\epsilon\rangle)$	-0.0344

there are no serious temporal resolution effects, and that the chosen cold-wire length is an optimal choice since we are interested in both small- and large-scale statistics of the temperature field.

Finally, all signals were high- and low-pass filtered and digitized using a 12-bit analog to digital converter. 4 or 8 $\times10^5$ data points were recorded for each record. The data were sampled slowly (with intervals on the order of an integral time period) for probability density function measurements, and rapidly (with intervals on the order of a Kolmogorov time period) for spectral (time-series) measurements. It is primarily the latter we use here.

Table I lists flow parameters at $x_1/M=62$—the furthest point downstream at which data was recorded. Turbulent quantities in this table were determined by subtracting, on a mean-square basis, the effect of the low-wave-number spikes present in the spectra (an artifact of the active grid). This is a more realistic description of the turbulence, and was described in detail by Mydlarski and Warhaft [6]. However, the structure functions presented in Sec. IV of this paper do contain contributions from the spikes. (It is less simple to eliminate their effect in physical space than in wave-number space.) These spikes occur at scales much larger than the integral scale (i.e., they occur at frequencies much smaller than those corresponding to the integral scale) and do not affect the turbulence [6,7].

III. THEORY

In this section, a generalized form of Yaglom's equation is developed by deriving the budget of $\langle(\Delta\theta)^2\rangle$, which is then integrated. The result is a modified version of Yaglom's equation that includes the effect of turbulent production and nonstationarities.

A. Budget of $\langle(\Delta\theta)^2\rangle$

Using a procedure similar to that of Monin and Yaglom [24], we write the advection-diffusion equation for the total temperature Θ at two points, $\vec{x}$ and $\vec{x}^+(=\vec{x}+\vec{r})$. $\vec{r}$ is an arbitrary vector equal to the separation between the two points. At the point $\vec{x}$ one can write

$$\partial_t\Theta+\tilde{u}_i\partial_{x_i}\Theta=\kappa\partial^2_{x_i}\Theta, \tag{8}$$

and at the point $\vec{x}^+=\vec{x}+\vec{r}$, one can write

$$\partial_t\Theta^++\tilde{u}_i^+\partial_{x_i^+}\Theta^+=\kappa\partial^2_{x_i^+}\Theta^+. \tag{9}$$

Repeated indices signify summation and $\tilde{u}_i$ and $\tilde{u}_i^+$ are instantaneous velocities at $\vec{x}$ and $\vec{x}^+$, respectively. We also remark that $\Theta=T+\theta$, where $T\equiv\langle\Theta\rangle$ and that $\tilde{\vec{u}}=\tilde{u}_i=U_i+u_i$, where $U_i\equiv\langle\tilde{u}_i\rangle$. Noting that (i) $\vec{G}=G_i=\partial_{x_i}T$, (ii) $\partial_{x_i}\tilde{u}_i^+=\partial_{x_i}\Theta^+=\partial_{x_i^+}\tilde{u}_i=\partial_{x_i^+}\Theta=0$ (since statistics measured in one frame of reference are independent of the coordinates of the other frame), (iii) $\partial_{x_i}\tilde{u}_i=\partial_{x_i^+}\tilde{u}_i^+=0$ (by conservation of mass for an incompressible flow), and (iv) in the flow under consideration, mean quantities are independent of the coordinate system in which they are written (i.e., $U_i^+=U_i$, $\overline{D}_t^+=\overline{D}_t=\partial_t+U_i\partial_{x_i}$,[5] $G_i^+=G_i$ and $\langle\epsilon_\theta^+\rangle=\langle\epsilon_\theta\rangle$), subtraction of Eq. (8) from Eq. (9) yields an equation for the increment of temperature fluctuations:[6]

$$\overline{D}_t\Delta\Theta+u_i^+\partial_{x_i^+}\Delta\Theta+u_i\partial_{x_i}\Delta\Theta=\kappa\partial^2_{x_i^+}\Delta\Theta+\kappa\partial^2_{x_i}\Delta\Theta. \tag{10}$$

After some manipulation, one obtains

$$\begin{aligned}&\partial_t\Delta T+\partial_t\Delta\theta+U_i\partial_{x_i}\Delta T+U_i\partial_{x_i}\Delta\theta+\Delta u_iG_i\\&\quad+\partial_{x_i^+}(\Delta u_i\Delta\theta)+u_i\partial_{x_i^+}\Delta\theta+u_i\partial_{x_i}\Delta\theta\\&\quad=\kappa\partial^2_{x_i^+}\Delta T+\kappa\partial^2_{x_i}\Delta T+\kappa\partial^2_{x_i^+}\Delta\theta+\kappa\partial^2_{x_i}\Delta\theta.\end{aligned} \tag{11}$$

We multiply Eq. (11) by $2\Delta\theta$ and (time) average to obtain[7]

$$\begin{aligned}&\partial_t\langle(\Delta\theta)^2\rangle+U_i\partial_{x_i}\langle(\Delta\theta)^2\rangle+2G_i\langle\Delta u_i\Delta\theta\rangle+\partial_{x_i^+}\langle\Delta u_i(\Delta\theta)^2\rangle\\&\quad+\partial_{x_i^+}\langle u_i(\Delta\theta)^2\rangle+\partial_{x_i}\langle u_i(\Delta\theta)^2\rangle\\&\quad=\kappa\partial^2_{x_i^+}\langle(\Delta\theta)^2\rangle-2\kappa\langle(\partial_{x_i^+}\Delta\theta)^2\rangle+\kappa\partial^2_{x_i}\langle(\Delta\theta)^2\rangle\end{aligned}$$

[5]Where $D_t=\partial_t+\tilde{u}_i\partial_{x_i}=\partial_t+U_i\partial_{x_i}+u_i\partial_{x_i}=\overline{D}_t+u_i\partial_{x_i}$ and similarly $D_t^+=\overline{D}_t+u_i^+\partial_{x_i^+}$.

[6]Differences between statistics at $\vec{x}^+$ and $\vec{x}$ are denoted by Δ [e.g., $\Delta\Theta\equiv\Theta^+-\Theta=\Theta(\vec{x}+\vec{r})-\Theta(\vec{x})$].

[7]Noting that $(\Delta\theta)\partial^2_{x_i}(\Delta\theta)=\partial_{x_i}[\Delta\theta\partial_{x_i}(\Delta\theta)]-[\partial_{x_i}(\Delta\theta)]^2=\frac{1}{2}\partial^2_{x_i}[(\Delta\theta)^2]-[\partial_{x_i}(\Delta\theta)]^2$.

$$-2\kappa\langle(\partial_{x_i}\Delta\theta)^2\rangle. \tag{12}$$

We can therefore write

$$\begin{aligned}\partial_t\langle(\Delta\theta)^2\rangle &+ U_i\partial_{x_i}\langle(\Delta\theta)^2\rangle + 2G_i\langle\Delta u_i\Delta\theta\rangle \\ &+ \partial_{x_i^+}\langle\Delta u_i(\Delta\theta)^2\rangle + (\partial_{x_i}+\partial_{x_i^+})\langle u_i(\Delta\theta)^2\rangle \\ &= \kappa(\partial_{x_i}^2+\partial_{x_i^+}^2)\langle(\Delta\theta)^2\rangle - 2\langle\epsilon_\theta^+\rangle - 2\langle\epsilon_\theta\rangle \\ &= \kappa(\partial_{x_i}^2+\partial_{x_i^+}^2)\langle(\Delta\theta)^2\rangle - 4\langle\epsilon_\theta\rangle. \end{aligned} \tag{13}$$

At this point, it is insightful to define a new variable [9] $\vec{X}$ as $\vec{X}\equiv(\vec{x}+\vec{x}^+)/2$, such that

$$\partial_{x_i^+}\langle\cdot\rangle \equiv \partial_{r_i}\langle\cdot\rangle + \frac{1}{2}\partial_{X_i}\langle\cdot\rangle, \quad \partial_{x_i}\langle\cdot\rangle \equiv -\partial_{r_i}\langle\cdot\rangle + \frac{1}{2}\partial_{X_i}\langle\cdot\rangle. \tag{14}$$

Consequently,

$$\partial_{X_i}\langle\cdot\rangle = \partial_{x_i} + \partial_{x_i^+}. \tag{15}$$

The result—in terms of the new variables $(\vec{r},\vec{X})$—is

$$\begin{aligned}\overline{D}_t\langle(\Delta\theta)^2\rangle &+ 2G_i\langle\Delta u_i\Delta\theta\rangle + \left(\partial_{r_i}+\frac{1}{2}\partial_{X_i}\right)\langle\Delta u_i(\Delta\theta)^2\rangle \\ &+ (\partial_{X_i})\langle u_i(\Delta\theta)^2\rangle = \kappa\left(2\partial_{r_i}^2+\frac{1}{2}\partial_{X_i}^2\right)\langle(\Delta\theta)^2\rangle - 4\langle\epsilon_\theta\rangle. \end{aligned} \tag{16}$$

As noted by Hill [9], in a locally homogeneous flow, all derivatives of statistics with respect to the new variable, $\vec{X}$ (i.e., $\partial_{X_i}\langle\cdot\rangle$) are negligible. It can be shown[8] that the nonhomogeneous turbulent and molecular transport terms are small in this flow. We could retain these terms in our analysis. However, since they are small and because the objective of this work is to examine the effect of gradient production (in addition to the decay) on the scalar fluctuations, we choose to omit these terms in our analysis. A further analysis, where the nonhomogeneous terms are significant [25] would be of merit.

In a fixed reference system, $\partial_t\langle\cdot\rangle\equiv 0$. We will still call term $U_i\partial_{x_i}\langle\rangle$ a ''decay term'' as it represents the decay of the turbulence (in a fixed frame of reference rather than one which moves with the mean flow). Neglecting the (small-scale) nonhomogeneous terms, one obtains

$$\begin{aligned}U_i\partial_{x_i}\langle(\Delta\theta)^2\rangle &+ \partial_{r_i}\langle\Delta u_i(\Delta\theta)^2\rangle + 2G_i\langle\Delta u_i\Delta\theta\rangle \\ &= 2\kappa\partial_{r_i}^2\langle(\Delta\theta)^2\rangle - 4\langle\epsilon_\theta\rangle. \end{aligned} \tag{17}$$

Due to the geometry of the flow under consideration, $|U_i|=U_1$ (since $U_2=U_3=0$) and $|G_i|=G_3=G$ since $(G_1=G_2\approx 0)$. Therefore, Eq. (17) can be rewritten as

$$\begin{aligned}U_1\partial_{x_1}\langle(\Delta\theta)^2\rangle &+ \partial_{r_i}\langle\Delta u_i(\Delta\theta)^2\rangle + 2G\langle\Delta u_3\Delta\theta\rangle \\ &= 2\kappa\partial_{r_i}^2\langle(\Delta\theta)^2\rangle - 4\langle\epsilon_\theta\rangle. \end{aligned} \tag{18}$$

B. Modified version of Yaglom's equation

Given the budget of $\langle(\Delta\theta)^2\rangle$ for the flow under consideration, it can be integrated to obtain a modified version of Yaglom's equation which accounts for the effects of production and non-stationarity.

We begin by assuming the isotropic form of the operator $\partial_{r_i}\equiv(2/r+\partial/\partial r)=(1/r^2)\partial_r(r^2\cdot)$. Multiplying Eq. (18) by r^2, integrating with respect to r and dividing by r^2, we obtain a version of Yaglom's equation that contains additional terms resulting from the mean temperature gradient, $\vec{G}$, and the nonstationarity:

$$\begin{aligned}-\langle\Delta u_1(\Delta\theta)^2\rangle &+ 2\kappa\frac{d}{dr}\langle(\Delta\theta)^2\rangle \\ &- \frac{1}{r^2}\int_0^r y^2[U_1\partial_{x_1}\langle(\Delta\theta)^2\rangle + 2G\langle\Delta u_3\Delta\theta\rangle]dy = \frac{4}{3}\langle\epsilon_\theta\rangle r. \end{aligned} \tag{19}$$

Here y is a dummy variable, representing the separation r. Equation (19) and its verification in Sec. IV are the principal results of this paper.[9] Denoting the new terms by D and P, the new equation is then written as

$$A+B+D+P=C, \tag{20}$$

where $C=4/3\langle\epsilon_\theta\rangle r$.

Term D represents the effect of the decay [or nonstationarity, which, as mentioned in Sec. I, can also be considered as a non-homogeneity in the streamwise (x_1) direction], and is given by

$$D(r) = -\frac{U_1}{r^2}\int_0^r y^2\partial_{x_1}\langle(\Delta\theta)^2\rangle dy. \tag{21}$$

The production term P is

[8]Measurements indicate that the nonhomogeneity in the viscous transport of scalar variance is dominated by its longitudinal component, i.e., $\partial_{x_i}^2\langle(\Delta\theta)^2\rangle \approx \partial_{x_1}^2\langle(\Delta\theta)^2\rangle$. In addition, it can be shown that the longitudinal component makes a much smaller contribution to the modified Yaglom's equation than the terms that will be retained. The nonhomogeneity in the turbulent transport of scalar variance, though larger than the nonhomogeneity of viscous transport, can also be shown to play a minimal role *in this flow* when compared to the other terms retained in our analysis.

[9]The large-scale (i.e., $r\to\infty$) and small-scale (i.e., $r\to 0$) limits of Eq. (19) are respectively discussed in Appendices A and B.

$$P(r) = -\frac{2G}{r^2}\int_0^r y^2 \langle \Delta u_3 \Delta\theta \rangle dy. \qquad (22)$$

The magnitudes of the terms in Eq. (19) are determined (experimentally) and presented in Sec. IV.

We now choose to make a few comments regarding the measurement of the new terms in our generalized form of Yaglom's equation. In its derivation, we have assumed an isotropic form of ∂_{r_i}. In an isotropic flow (such as decaying grid turbulence) with isotropic temperature fluctuations (generated by a mandoline, as in Danaila *et al.* [4]), such an assumption is readily made. In the present work, the effect of production on the scalar fluctuations is of interest. By definition, for production of scalar fluctuations to occur, the flow must be anisotropic (since a mean scalar gradient must be present). However, we are able to justify the assumption of the isotropic form of the gradient operator as follows.

Since turbulent advection and molecular diffusion terms correspond to small-scale motions, we assume they are locally isotropic and will therefore only depend on the modulus $r = |\vec{r}|$. For simplicity, we measure r along the x_1 axis.

The decay term D is a large-scale, nonhomogeneous term (see Ref. [4] for further physical explanations). The second-order scalar structure functions are not necessarily isotropic in a flow with a mean scalar gradient. They are approximately isotropic for relatively large scales, where $\langle(\Delta\theta)^2\rangle(r_1) \approx \langle(\Delta\theta)^2\rangle(r_3) \approx 2\langle\theta^2\rangle$. At the smallest separations, the longitudinal and transverse second-order structure functions differ by a factor 1.4. This latter result derives from the already mentioned fact that $\langle(\partial_{x_3}\theta)^2\rangle / \langle(\partial_{x_1}\theta)^2\rangle \approx 1.2 - 1.4$ [7]. However, since the decay term is only significant at the largest scales [4], it can be well approximated as depending solely on r (again, measured along the x_1 axis for simplicity).

The production term P is not isotropic. Were this term isotropic, replacement of u_3 by (for instance) u_1, would not change the value of P. (This is not the case: $|\langle u_1\theta\rangle| \ll |\langle u_3\theta\rangle|$ [19,26].) However, in the limit of large scales, the directional differences in this term disappear, since $\lim_{|r|\to\infty} P(\vec{r}) = 4G\langle u_3\theta\rangle$, regardless of the orientation of $\vec{r}$. For small scales, the value of P depends slightly on the spatial direction, as observed in Fig. 1. It will be shown below that the contribution of P to Eq. (19) decreases with scale size. Therefore, it is a reasonable approximation to evaluate $P(\vec{r})$ using only one spatial direction (x_1), since its contribution is significant only at large scales.

IV. RESULTS

Figure 2 represents terms in Eq. (20), divided by term C. The supplementary contribution, $S/C = (D+P)/C$, is positive for all scales and increases in importance for larger and larger scales. The ratios $(A+B)/C$ and $(A+B+S)/C$ of the terms appearing in Eq. (20) are to be compared with the wide solid line (which is equal to 1 for all scales). While the classical Yaglom equation (1) is verified to within 15% for small scales, and worsens significantly for larger and larger scales, the modified equation maintains approximately the same level of precision for all scales.

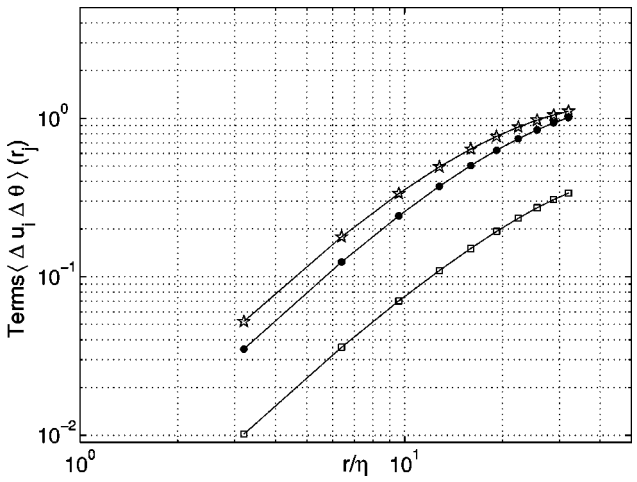

FIG. 1. Longitudinal and transverse ''heat flux structure functions.'' $\langle\Delta u_3(\Delta\theta)\rangle(r_1)$ (⋆), $\langle\Delta u_3(\Delta\theta)\rangle(r_3)$ (●), and $\langle\Delta u_1(\Delta\theta)\rangle(r_1)$ (□). These are DNS results graciously provided by A. Pumir.

At the smallest scales, the supplementary contribution S is negligible, and Eq. (19) reduces to Eq. (6). In this flow, Eq. (6) is not verified because of the small-scale anisotropy of a passive scalar in flows with a mean scalar gradient. As mentioned in Sec. I, the ''total'' scalar dissipation is therefore different from the value obtained when local isotropy is assumed. Therefore, in the limit of $r \to 0$, $(A+B+S)/C$ tends to a value less than one due to the nonisotropic definition of $\langle\epsilon_\theta\rangle$ used in estimating term C. In this limit, $(A+B+S)/C$ should tend to $\langle\epsilon_\theta\rangle_{iso} / \langle\epsilon_\theta\rangle = 3/3.4 = 0.88$, which it does, to within experimental error.

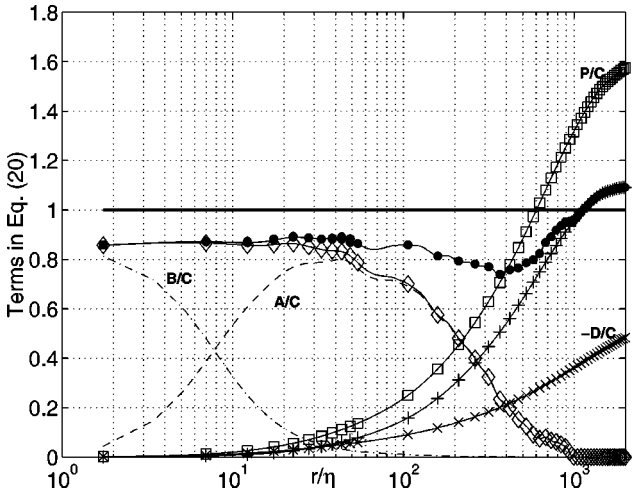

FIG. 2. The nondimensionalized terms in the generalized form of Yaglom's equation [Eqs. (19) and (20)]: $(A+B+D+P)/C = 1$) as a function of longitudinal separation. The sum of A/C (dashed line) and B/C (dot-dashed line)—Yaglom's original equation—is represented by ◇. The P/C source term is given by □, $-D/C$ by ×, and their sum $(S/C = (D+P)/C)$ by +. The sum of all the terms $[(A+B+S)/C]$ is given by ●.

For larger scales (where the supplementary contributions begin to take effect), term P is positive, as must be the case, since the turbulent heat flux in the direction of the gradient is negative (and therefore so must be $\langle \Delta u_3 \Delta\theta \rangle$). In the flow under consideration, term D is negative since $\partial_{x_1}\langle(\Delta\theta)^2\rangle > 0$, so that temperature fluctuations increase in the downstream direction. This is a direct consequence of the presence of the mean scalar gradient $\vec{G}$, which constitutes a continuous injection of scalar fluctuations in this flow.

In the limit of large separations, it is shown in Appendix A that Eq. (19) is equivalent to the one-point scalar variance budget. Hence the generalized version of Yaglom's equation tends toward 1 for large separations, as it should. At these large scales, the ratio of the magnitudes of the production term (P) and the nonstationary term (D) is about 3, in agreement with the result obtained for the corresponding terms in the scalar variance budget. (Also see Fig. 4 for the position $x_1/M = 62$ in Appendix A.)

In Danaila *et al.* [4], the scalar field was isotropic, and the nonstationarity was the only large-scale mechanism in this flow. Consequently, the nonstationarity dominated the generalized Yaglom's equation at large scales. [In Danaila *et al.*, Eq. (4) was verified to within $\pm 10\%$ over the range of scales investigated.] The present study involves two large-scale mechanisms (production and nonstationarity). This, combined with the small-scale anisotropy arising from the mean temperature gradient, resulted in a less accurate balance of Eq. (19) than obtained by Danaila *et al.*

Figure 2 indicates that, in this flow, the transfer of scalar variance is dictated not only by turbulent advection and molecular dissipation, but also by turbulent production and nonstationarity. These mechanisms should be taken into account not only in the one-point scalar variance budget, but in the higher-order moment balances of all flows characterized by a moderate Reynolds number and fed by a mean-temperature gradient.

V. CONCLUSIONS

A generalized form of Yaglom's equation was derived for the case of decaying grid turbulence with an imposed mean temperature gradient. The large-scale motion is characterized by two phenomena: the nonstationarity of turbulent temperature fluctuations and their production by a mean temperature gradient $\vec{G}$. (In this flow, the nonhomogeneous terms associated with the turbulent and viscous transport of temperature variance were not found to play a significant role.) The effects relating to the production and nonstationarity of temperature fluctuations are mathematically expressed as two new terms in Yaglom's equation. The generalized Yaglom's equation (19) is well satisfied over an extended range of scales, particularly for the largest scales. This result emphasizes the role played by the large-scale motion, herein decomposed into two separate effects. However, the effect of the persistent anisotropy of passive scalars in flows with a mean scalar gradient (resulting in $\langle \epsilon_\theta \rangle \neq \langle \epsilon_\theta \rangle_{iso}$) is observed. Such an anisotropy is inconsistent with the implicit assumption of local isotropy in the derivation of Yaglom's equation. Its effect cannot be ''solved'' nor explained by such an approach, and requires further efforts.

ACKNOWLEDGMENTS

F. Anselmet and Z. Warhaft are gratefully acknowledged for their help. A. Pumir and E. Lindborg are also warmly thanked for fruitful discussions. Support was provided by the Fonds pour la Formation de Chercheurs et l'Aide à la Recherche, the Natural Sciences and Engineering Research Council of Canada, and the U.S. Department of Energy (Basic Energy Sciences). The collaboration between L.D. and L.M. was initiated by a *Bourse d'excellence pour un stage de recherche scientifique* from the Ministère de l'Éducation du Québec.

APPENDIX A: LARGE-SCALE LIMIT OF EQ. (19)

Equation (19) is examined in the limit of large scales (i.e., $r \to \infty$). As already explained in Ref. [4],

$$\lim_{r\to\infty} D = \lim_{r\to\infty} -\frac{U_1}{r^2}\int_0^r y^2 \partial_{x_1}\langle(\Delta\theta)^2\rangle dy$$

$$= \lim_{r\to\infty} -\frac{U_1}{r^2}\left[\int_0^l y^2 \partial_{x_1}\langle(\Delta\theta)^2\rangle dy + \int_l^r y^2 \partial_{x_1}\langle(\Delta\theta)^2\rangle dy\right],$$

where l is the integral length scale of the turbulence, defined [6] as $l \equiv 0.9\langle u^2\rangle^{3/2}/\langle\epsilon\rangle$.

For $r \to \infty$, $\int_0^l y^2 \partial_{x_1}\langle(\Delta\theta)^2\rangle dy \ll \int_l^r y^2 \partial_{x_1}\langle(\Delta\theta)^2\rangle dy$, since the first integral has a finite value while the second one tends to infinity, *viz.* $\lim_{r\to\infty}\partial_{x_1}\langle(\Delta\theta)^2\rangle = 2\partial_{x_1}\langle\theta^2\rangle$ is finite while y^2 is continuously increasing. Thus, for $r \gg l$, one can make the approximation $\langle(\Delta\theta)^2\rangle \approx 2\langle\theta^2\rangle$, so that

$$\lim_{r\to\infty} D \simeq -\frac{U_1}{r^2}\int_l^r y^2 \partial_{x_1}\langle(\Delta\theta)^2\rangle dy \approx -\frac{2U_1}{3}\partial_{x_1}\langle\theta^2\rangle r.$$

In a similar manner, one obtains

$$\lim_{r\to\infty} P = \frac{4}{3} G\langle u_3\theta\rangle r. \tag{A1}$$

Given that

$$\lim_{r\to\infty} A = \lim_{r\to\infty} B = 0, \tag{A2}$$

Eq. (19) reduces to the one-point scalar variance budget:

$$U_1\partial_{x_1}\langle\theta^2\rangle/2 + G\langle u_3\theta\rangle = -\langle\epsilon_\theta\rangle. \tag{A3}$$

A nondimensional form of Eq. (A3) is obtained by dividing both sides by $-\langle\epsilon_\theta\rangle$, which can be written symbolically as

$$I + II = 1. \tag{A4}$$

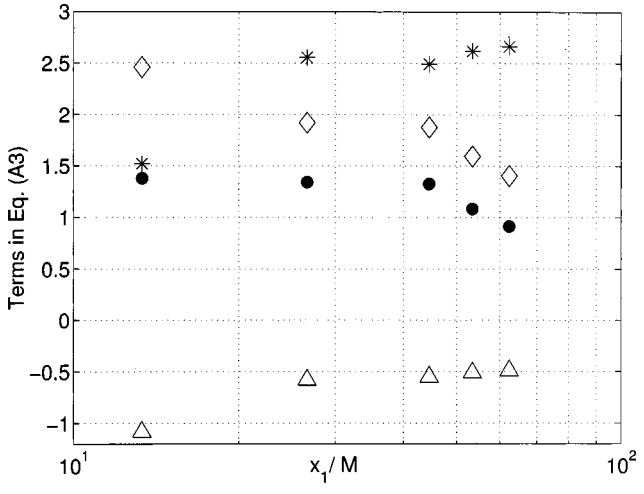

FIG. 3. Terms in Eq. (A3) and (A4) as functions of downstream position. $I=-U_1\partial_{x_1}\langle\theta^2\rangle/[2\langle\epsilon_\theta\rangle]$ ($\triangle$), $II=-G\langle u_3\theta\rangle/\langle\epsilon_\theta\rangle$ ($\diamond$), and terms $I+II$ ($\bullet$). * represents the variation of $2\langle\epsilon_\theta\rangle/G^2M^2$.

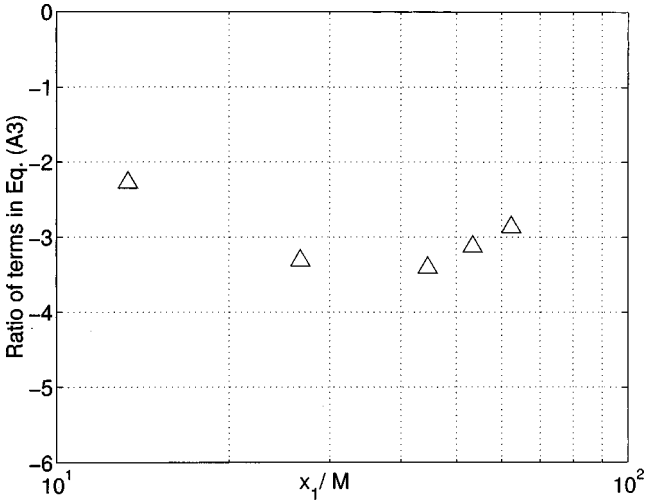

FIG. 4. Ratio of the production to nonstationary terms (II/I) in Eqs. (A3) and (A4).

Terms I and II are shown as a function of downstream-distance in Fig. 3. Term I represents the nonstationarity and term II represents the turbulent production. The former term is negative (since $\partial_{x_1}\langle\theta^2\rangle$ is positive in the flow under consideration). Its magnitude decreases with x_1 to approximately 0.5 at $x_1/M=62$. Term II is positive and larger than 1, but tends toward 1 for the furthest downstream positions.

At the two furthest downstream positions, the sum of terms I and II is equal to 1 (to within $\pm 10\%$), indicating that the production and decay terms balance the scalar dissipation. In other words, the turbulent transport of scalar variance has a small role at the large scales far enough away from the grid. Note that the flow under consideration has been previously investigated (e.g., Sirivat and Warhaft [19] and Overholt and Pope [26]). In Ref. [19], the one-point energy budget was also balanced with a precision of $\pm 10\%$–see Fig. 18 of this paper. The nonhomogeneous advection term, $\partial_i\langle u_i\theta^2\rangle$, is negligible, since $\partial_3\langle u_3\theta^2\rangle\approx 0$—see Fig. 11 and the comments in Ref. [19]. (Note that Fig. 11 of Ref. [19] presents results for a case where the mean temperature gradient is generated by a mandoline. The results may differ for a mean temperature gradient generated by a toaster.)

We remark that in Fig. 3, $I+II\approx 0.9$. However, for the largest values of r shown in Fig. 2 $(A+B+S)/C\approx 1.1$ (at $x/M=62$). This is because at $r=2000\eta$, θ and θ^+ are not yet completely uncorrelated. In the limit of $r/\eta\to\infty$, θ and θ^+ decorrelate and $(A+B+S)/C$ must then become equal to $I+II$.

Figure 4 represents the ratio of the production and nonstationary terms in Eq. (A4) (i.e., II/I), which is approximately -3 for a large range of positions behind the grid. This value is in agreement with $\lim_{r\to\infty}P(r)/D(r)\approx -3$, as can be observed in Fig. 2.

APPENDIX B: SMALL-SCALE LIMIT OF EQ. (19)

It is of interest to study what Eq. (19) becomes in the limit of small scales ($r\to 0$). In this limit, $\langle(\Delta\theta)^2\rangle$ can be approximated, using a Taylor series expansion up to order r^4, by

$$\langle(\Delta\theta)^2\rangle\simeq\left\langle\left(\frac{\partial\theta}{\partial x_1}\right)^2\right\rangle r^2-\frac{1}{12}\left\langle\left(\frac{\partial^2\theta}{\partial x_1^2}\right)^2\right\rangle r^4. \qquad \text{(B1)}$$

Assuming isotropy, one can write

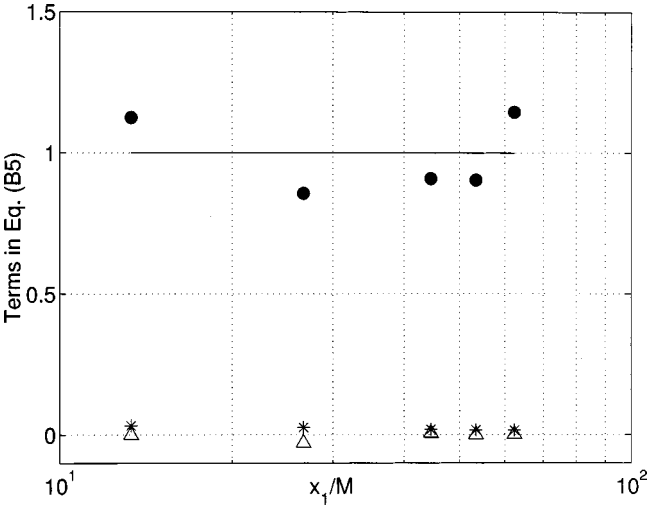

FIG. 5. Terms in Eq. (B5):

$$-\frac{U_1}{15\kappa}\frac{\partial\langle\epsilon_\theta\rangle_{iso}}{\partial x_1}\Big/\,2\frac{\kappa}{3}\left\langle\left(\frac{\partial^2\theta}{\partial x_1^2}\right)^2\right\rangle\ (\triangle),$$

$$-\frac{2G}{5}\left\langle\frac{\partial u_3}{\partial x_1}\cdot\frac{\partial\theta}{\partial x_1}\right\rangle\Big/\,2\frac{\kappa}{3}\left\langle\left(\frac{\partial^2\theta}{\partial x_1^2}\right)^2\right\rangle\ (*),$$

and

$$-\left\langle\left(\frac{\partial u_1}{\partial x_1}\right)\left(\frac{\partial\theta}{\partial x_1}\right)^2\right\rangle\Big/\,2\frac{\kappa}{3}\left\langle\left(\frac{\partial^2\theta}{\partial x_1^2}\right)^2\right\rangle\ (\bullet).$$

$$\frac{\partial}{\partial x_1}\langle(\Delta\theta)^2\rangle \simeq \frac{r^2}{3\kappa}\frac{\partial}{\partial x_1}\langle\epsilon_\theta\rangle_{iso}. \tag{B2}$$

Similarly,

$$\langle \Delta u_3 \Delta\theta\rangle \simeq \left\langle \frac{\partial u_3}{\partial x_1}\frac{\partial\theta}{\partial x_1}\right\rangle r^2,$$

$$\langle \Delta u_1(\Delta\theta)^2\rangle \simeq \left\langle \frac{\partial u_1}{\partial x_1}\left(\frac{\partial\theta}{\partial x_1}\right)^2\right\rangle r^3. \tag{B3}$$

Using relations (B1)–(B3), the supplementary terms in Eq. (19) become

$$-\frac{U_1}{r^2}\int_0^r y^2\frac{\partial}{\partial x_1}\langle(\Delta\theta)^2\rangle dy$$

$$= -\frac{U_1}{r^2}\frac{\partial}{\partial x_1}\left\langle\left(\frac{\partial\theta}{\partial x_1}\right)^2\right\rangle\int_0^r y^2 y^2 dy = -\frac{U_1}{15\kappa}\frac{\partial\langle\epsilon_\theta\rangle_{iso}}{\partial x_1}r^3,$$

$$-\frac{2G}{r^2}\int_0^r y^2\langle\Delta u_3\Delta\theta\rangle dy \simeq -\frac{2G}{5}\left\langle\frac{\partial u_3}{\partial x_1}\cdot\frac{\partial\theta}{\partial x_1}\right\rangle r^3. \tag{B4}$$

Substitution of the above expressions into Eq. (19), replacing $\langle\Delta u_1(\Delta\theta)^2\rangle$ by $\langle(\partial u_1/\partial x_1)(\partial\theta/\partial x_1)^2\rangle r^3$ and equating terms in r^3, one obtains

$$-\frac{U_1}{15\kappa}\frac{\partial\langle\epsilon_\theta\rangle_{iso}}{\partial x_1} - \frac{2G}{5}\left\langle\frac{\partial u_3}{\partial x_1}\cdot\frac{\partial\theta}{\partial x_1}\right\rangle = \left\langle\left(\frac{\partial u_1}{\partial x_1}\right)\left(\frac{\partial\theta}{\partial x_1}\right)^2\right\rangle + \frac{2\kappa}{3}\left\langle\left(\frac{\partial^2\theta}{\partial x_1^2}\right)^2\right\rangle. \tag{B5}$$

Equation (B5) is the transport equation for $\langle\epsilon_\theta\rangle_{iso}$. It is analogous to the transport equation for $\langle\epsilon\rangle$ (or, equivalently, the enstrophy $\langle\omega^2\rangle$), as first written by Batchelor and Townsend [27]. The transport equation for $\langle\epsilon_\theta\rangle$ was previously studied [28–30] in decaying, isotropic grid turbulence heated by a mandoline. (There the budget of $\langle\epsilon_\theta\rangle_{iso}$ was simpler since a mean scalar gradient was not present.) These studies only considered the first term on the left hand side and the two terms on the right hand side of Eq. (B5).

In the flow under consideration, both terms on the left hand side of Eq. (B5) are small with respect to the dissipative term, $2\kappa\langle(\partial^2_{x_1}\theta)^2\rangle/3$, as can be seen in Fig. 5.

This result is different with respect to the one obtained in (standard) grid turbulence without a mean scalar gradient [28], where the role of the nonstationary term was found to be very important in the balance of Eq. (B5). In our case, equation (B5) is balanced ($\pm 15\%$; see Fig. (5)) by the terms on the right-hand side. This result is attributed to the presence of the passive scalar production term, which constitutes the only difference between this flow and classical grid turbulence with isotropic temperature fluctuation generated by a mandoline, and the higher Reynolds number of the present flow.

[1] A. M. Yaglom, Dokl. Akad. Nauk. SSSR **69**, 743 (1949).
[2] A. N. Kolmogorov, Dokl. Akad. Nauk. SSSR **30**, 301 (1941).
[3] A. N. Kolmogorov, Dokl. Akad. Nauk. SSSR **32**, 16 (1941).
[4] L. Danaila, F. Anselmet, T. Zhou, and R. A. Antonia, J. Fluid Mech. **391**, 359 (1999).
[5] R. A. Antonia, A. J. Chambers, and L. W. Browne, Exp. Fluids **1**, 213 (1983).
[6] L. Mydlarski and Z. Warhaft, J. Fluid Mech. **320**, 331 (1996).
[7] L. Mydlarski and Z. Warhaft, J. Fluid Mech. **358**, 135 (1998).
[8] U. Frisch, *Turbulence: the Legacy of A.N. Kolmogorov* (Cambridge University Press, Cambridge, 1995).
[9] R. J. Hill, J. Fluid Mech. **353**, 67 (1997).
[10] E. Lindborg, Phys. Fluids **11**, 510 (1999).
[11] F. Moisy, P. Tabeling, and H. Willaime, Phys. Rev. Lett. **82**, 3994 (1999).
[12] Z. Warhaft and J. L. Lumley, J. Fluid Mech. **88**, 659 (1978).
[13] K. R. Sreenivasan, Proc. R. Soc. London, Ser. A **434**, 165 (1991).
[14] C. Tong and Z. Warhaft, Phys. Fluids **6**, 2165 (1994).
[15] A. Pumir, Phys. Fluids **6**, 2118 (1994).
[16] M. Holzer, and E. D. Siggia, Phys. Fluids **6**, 1820 (1994).
[17] K. Yoon and Z. Warhaft, J. Fluid Mech. **215**, 601 (1990).
[18] H. Makita, Fluid Dyn. Res. **8**, 53 (1991).
[19] A. Sirivat and Z. Warhaft, J. Fluid Mech. **128**, 323 (1983).
[20] S. Corrsin, J. Appl. Phys. **23**, 113 (1952).
[21] L. W. B. Browne, R. A. Antonia, and L. P. Chua, Exp. Fluids **7**, 201 (1989).
[22] J. H. Lienhard, Ph.D. dissertation, University of California at San Diego, 1988.
[23] J. Haughdal, and J. H. Lienhard, J. Phys. E **21**, 167 (1988).
[24] A.S. Monin and A.M. Yaglom, *Statistical Fluid Mechanics* (MIT Press, Cambridge, MA, 1975).
[25] L. Danaila, F. Anselmet, T. Zhou, and R. A. Antonia, J. Fluid Mech. **430**, 87 (2001).
[26] M. R. Overholt and S. B. Pope, Phys. Fluids **8**, 3128 (1996).
[27] G. K. Batchelor and A. A. Townsend, Proc. R. Soc. London, Ser. A **190**, 534 (1947).
[28] T. Zhou, R. A. Antonia, L. Danaila, and F. Anselmet, Exp. Fluids **28**, 143 (2000).
[29] M. Lesieur, *Turbulence in Fluids*, 3rd ed. (Kluwer, Dordrecht, 1997).
[30] M. Gonzalez and A. Fall, Phys. Fluids **10**, 654 (1998).